International Journal of Engineering Research & Technology (IJERT)
ISSN: 2278-0181
Vol. 6 Issue 06, June - 2017

Random Dynamic Response Analysis of Bridge Subjected to Moving Vehicles

Xuan-Toan Nguyen[#1]
Faculty of Road and Bridge Engineering,
University of Danang - University of Science and Technology, Danang City, Vietnam

Kuriyama Yukihisa[#2]
Research into Artifacts,
Center for Engineering,
The University of Tokyo, Japan

Duy-Thao Nguyen[#3]
Faculty of Road and Bridge Engineering,
University of Danang
University of Science and Technology,
Danang City, Vietnam

***Abstract*-- This article presents random vibration analysis of dynamic vehicle-bridge interaction due to road unevenness based on the Finite element method and Monte-Carlo simulation method. The road unevenness are described by a zero-mean stationary Gaussian random process. The vehicle is a dumper truck with three axles. Each axle of vehicle is idealised as two mass dynamic system, in which a mass is supported by a spring and a dashpot. The structural bridge are two-span slab beam concrete, are simulated as bending beam elements. The finite element method is applied to established the overall model of vehicle-bridge interaction. Galerkin method and Green theory are used to discrete the motion equation of vehicle-bridge system in space domain. Solutions of the motion equations are solved by mean of Runge-Kutta-Mersion method (RKM) in time domain. The numerical results are in good agreement with full-scale field testing results of the slab beam concrete at NguyenTriPhuong bridge in Danang city, Vietnam. Also, the effects of road surface condition on dynamic impact factor of bridge are investigated detail. The numerical results show that dynamic impact factor of bridge has increased significantly when road unevenness have varied from Grade A-road to Grade E-road according to ISO 8608:1995 [1]"Mechanical vibration - Road surface profiles – Reporting of measured data".**

Keywords*-- *Monte-Carlo simulation method, finite element method, road unevenness, moving vehicles, vehicle-bridge interaction, slab beam concrete.

I. INTRODUCTION

Vehicle-bridge interaction has been a subject of significant research for a long time. The aim of these studies is to investigate the structural behaviour of bridge under moving vehicles, as well as the ride comfort of vehicles travelling a bridge. Dynamic vehicle-bridge interaction results in a increase or decrease of the bridge deformation, which is described by the dynamic impact factor (IM) or the dynamic amplification factor (DAF) or dynamic load allowance (DLA) that reflects how many times the constant load must be multiplied to cover additional dynamic effects, Frýba [2]. The dynamic IM plays a vital role in the practice of bridge design and condition assessment. Accurate evaluation of IMs will lead to safe and economical designs for new bridges and provide valuable information for condition assessment and management of existing bridges.

Honda et al. [3] derived the power spectral density (PSD) of road surface roughness on 56 highway bridges, measured using a surveyor's level. For each bridge, 84 lines at 10-20 cm intervals and 0.5 and 2.0 m from the centerline of the road were measured. The authors observed that the PSD of roadway roughness can be approximated by an exponential function, and proposed different functions for certain bridge structural systems. Palamas et al. [4], Coussy et al. [5] presented a theoretical study of the effects of surface road unevenness on the dynamic response of bridges under suspended moving loads. A single-degree-of-freedom system was used for the vehicle and a Rayleigh-Ritz method was used for the dynamic analysis. This study showed that in some cases, the DAF could be two to three times that recommended by current international design codes, suggesting that road unevenness could no longer be neglected. Inbanathan and Wieland [6] presented an analytical investigation on the dynamic response of a simply supported box girder bridge due to a moving vehicle. In particular, they considered the profile of the roadway using a response spectrum and 10 artificially generated time history loads for speeds of 19 and 38 km/h. The study of the response of a bridge due to a generated dynamic force was justified in view of the random nature of the problem. Some of the findings reported were the following: 1-The effect of vehicle mass on the bridge response is more significant for high speeds; 2-The maximum response is not affected by damping; 3- The stresses developed by a heavy vehicle moving over a rough surface at high speeds exceed those recommended by current bridge design codes. Hwang and Nowak [7] presented a procedure to calculate statistical parameters for dynamic loading of bridges, to be used in design codes. These parameters, based on surveys and tests, included vehicle mass, suspension system and tires, and roadway roughness, which was simulated by stochastic processes. This procedure was applied to steel and prestressed concrete girder bridges, for single and side-by-side vehicle configurations. Values of the DAF were computed using prismatic beam models for the bridges and step-by-step integrations. It was found that: 1-the DAF decreases with an increase in vehicle weight; 2- the DAF for two side-by-side vehicles is lower than that for a single vehicle; and 3- the dynamic load is generally uncorrelated with the static live load. But the vehicle model of Hwang and Nowak didn't consider the dashpot of suspension system and tires. Au et al.

International Journal of Engineering Research & Technology (IJERT)
ISSN: 2278-0181
Vol. 6 Issue 06, June - 2017

[8] presented a numerical study of the effects of surface road unevenness and long-term deflection on the dynamic impact factor of prestressed concrete girder and cable-stayed bridges due to moving vehicles. The results showed that the effects of random road unevenness and the long-term deflection of concrete deck on bridge vary a lot at the sections closed to the bridge tower, with significant effects on the short cables. Lombaert and Conte [9] proposed the random vibration analysis of dynamic vehicle-bridge interaction due to road unevenness by an original frequency domain method. The road unevenness was modeled by the random nonstationary process. Due to the complexity of the problem, the authors presented only the results of simple supported beam model subjected to a moving concentrated load. Xuan-Toan Nguyen et al. [10],[11] and [12] analyzed the dynamic three-axle vehicle - bridge interaction considering the change of vehicle velocity through braking force by finite element method. The numerical results showed that the influence of braking force has effects significantly on dynamic impact factor of bridge. However, most of the previous research studied on dynamic interaction between the vehicle and simply supported bridge, very few studies have focused on the multi-span slab beam bridge with link deck considering the random road unevenness effects. Additionally, the full-scale field test is needed in order to obtain a clearer understanding of the relationship between dynamic interaction for bridge types and vehicle models.

This study develops the FEM to analyze the random dynamic interaction between three-axle dumper truck vehicle and two-span prestressed slab beam bridge with link deck due to road unevenness. The road unevenness is simulated by a zero-mean stationary Gaussian random process. The bridge is modelled by finite element method. The dumper-truck has three axles. Each axle is idealised by two mass, in which a mass is supported by a spring and dashpot. The governing equation of random dynamic vehicle-bridge interaction is derived by means of dynamic balance principle. Galerkin method and Green theory are employed to discrete the governing equation in space domain. The solutions of equation are solved by Runge-Kutta-Mersion method. Monte-Carlo simulation is applied to generate the random road unevenness input. The numerical results are in good agreement with full-scale field test results of two-span prestressed slab beam at Nguyen-Tri-Phuong bridge in Danang city, Vietnam. Also, the effects of the road surface condition on dynamic impact factor of the prestressed slab beam bridge are discussed.

II. THE MODEL OF VEHICLE-BRIDGE INTERACTION

Consider a two-span slab beam with link deck subjected to a three-axle dumper truck vehicle as in Fig. 1. Assume that the body weight of vehicle and goods on the vehicle distribute to three axle m_{11}, m_{12} and m_{13}, respectively. The mass of three axles are m_{21}, m_{22} and m_{23} respectively. The dynamic interaction model between a three-axle vehicle and a girder element is described as in Fig. 2.

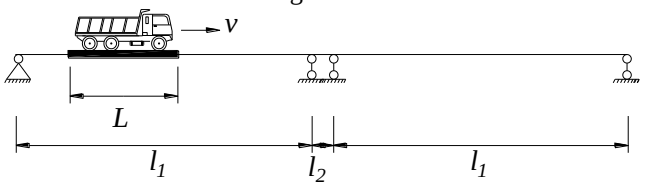

Fig 1. Schematic of vehicle moving on bridge

where $w_i(x_i,t)$ is the vertical displacement of girder element at ith axle of vehicle; r_i is road unevenness at ith axle of vehicle; z_{1i} is the vertical displacement of chassis at ith axle of vehicle; z_{2i} is the vertical displacement of ith axle of vehicle; y_{1i} is the relative displacement between the chassis and ith axle; y_{2i} is the relative displacement between ith axle and girder element; $G_i.\sin\psi_i$ is the engine excitation force at ith axle, it is assumed as a harmonic function ; k_{1i} and d_{1i} are the spring and dashpot of suspension at ith axle respectively; k_{2i} and d_{2i} are the spring and dashpot of tire at ith axle respectively; x_i is the coordinate of the ith axle of the vehicle at time t (i=1, 2, 3).

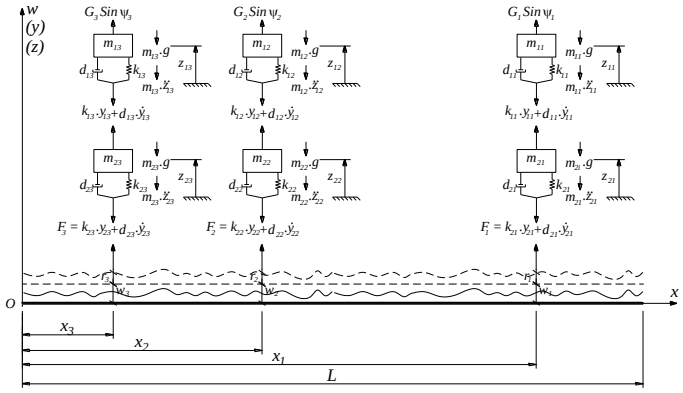

Fig 2. Schematic of vehicle-bridge interaction

Base on the model of dynamic vehicle-bridge interaction in Fig.2 and using d'Alembert's principle, the dynamic equilibrium of each mass m_{1i}, m_{2i} on the vertical axis can be written as follows:

$$m_{1i}.\ddot{z}_{1i}+d_{1i}.\dot{z}_{1i}-d_{1i}.\dot{z}_{2i}+k_{1i}.z_{1i}-k_{1i}.z_{2i}=G_i.\sin\psi_i-m_{1i}.g \quad (1)$$

$$\begin{aligned} m_{2i}.\ddot{z}_{2i}-d_{1i}.\dot{z}_{1i}+(d_{1i}+d_{2i}).\dot{z}_{2i}-k_{1i}.z_{1i}+(k_{1i}+k_{2i}).z_{2i} \\ =k_{2i}(w_i+r_i)+d_{2i}.(\dot{w}_i+\dot{r}_i)-m_{2i}.g \end{aligned} \quad (2)$$

where $\dot{r}_i$ is the first derivation of road unevenness at ith axle of vehicle. Adding on the logic control function, Eq.(1) and (2) can be rewritten as follows:

$$\begin{aligned} \xi_i(t).[m_{1i}.\ddot{z}_{1i}+d_{1i}.\dot{z}_{1i}-d_{1i}.\dot{z}_{2i}+k_{1i}.z_{1i}-k_{1i}.z_{2i}] \\ =\xi_i(t).[G_i.\sin\psi_i-m_{1i}.g] \end{aligned} \quad (3)$$

$$\begin{aligned} \xi_i(t)[m_{2i}.\ddot{z}_{2i}-d_{1i}.\dot{z}_{1i}+(d_{1i}+d_{2i})\dot{z}_{2i}-k_{1i}.z_{1i}+(k_{1i}+k_{2i})z_{2i}] \\ =\xi_i(t)[k_{2i}(w_i+r_i)+d_{2i}.(\dot{w}_i+\dot{r}_i)-m_{2i}.g] \end{aligned} \quad (4)$$

$$\xi_i(t)=\begin{cases} 1 & if \quad t_i\le t\le t_i+T_i \quad ; \quad T_i=\dfrac{L}{v} \\ 0 & if \quad t<t_i \quad and \quad t>t_i+T_i \end{cases} \quad (5)$$

From Fig.2, the contact force between the ith axle and girder element is described by:

$$F_i=k_{2i}.y_{2i}+d_{2i}.\dot{y}_{2i} \quad (6)$$

The combined Eq.(1),(2),(5) and (6), the contact force between the ith axle and girder element can be rewritten as follows:

$$\begin{aligned} p_i(x,z,t)=\xi_i(t)\times \\ [G_i.\sin\psi_i-(m_{1i}+m_{2i}).g-m_{1i}.\ddot{z}_{1i}-m_{2i}.\ddot{z}_{2i}].\delta(x-x_i) \end{aligned} \quad (7)$$

where $\delta(x-x_i)$ is the Dirac delta function.

International Journal of Engineering Research & Technology (IJERT)
ISSN: 2278-0181
Vol. 6 Issue 06, June - 2017

According to Ray [13], the governing equation for the vibration of damped girder due to uniform loading *p(x, z, t)* can be written as follow:

$$EJ.\left(\frac{\partial^4\omega}{\partial x^4}+\theta\frac{\partial^5\omega}{\partial x^5.\partial t}\right)+\rho_m.\frac{\partial^2\omega}{\partial t^2}+\beta.\frac{\partial\omega}{\partial t}=p(x,z,t) \quad (8)$$

$$p(x,z,t)=\sum_{i=1}^{n}\xi_i(t)\times \quad (9)$$
$$\left[G_i.\sin\psi_i-(m_{1i}+m_{2i}).g-m_{1i}.\ddot{z}_{1i}-m_{2i}.\ddot{z}_{2i}\right].\delta(x-x_i)$$

where *EJ* is the bending stiffness of girder element; θ and β are the coefficient of internal friction and external friction of girder element; ρ_m is the mass of girder per unit length; n is the number of axle (n=3).

The Galerkin method and Green theory are applied to Eq. (3), (4) and (8) transform into matrix form, and the differential equations of girder element can be written in a matrix form as follow:

$$[M_e].\{\ddot{q}\}+[C_e].\{\dot{q}\}+[K_e].\{q\}=\{f_e\} \quad (10)$$

where $\{\dot{q}\}$, $\{q\}$, $\{q\}$, $\{f_e\}$ are the complex acceleration vector, complex velocity vector, complex displacement vector, complex forces vector, respectively.

$$\{\ddot{q}\}=\begin{Bmatrix}\ddot{w}\\ \ddot{z}_1\\ \ddot{z}_2\end{Bmatrix};\{\dot{q}\}=\begin{Bmatrix}\dot{w}\\ \dot{z}_1\\ \dot{z}_2\end{Bmatrix};\{q\}=\begin{Bmatrix}w\\ z_1\\ z_2\end{Bmatrix};\{f_e\}=\begin{Bmatrix}F_w\\ F_{z1}\\ F_{z2}\end{Bmatrix} \quad (11)$$

$$\{w\}=\begin{Bmatrix}w_{y1}\\ \varphi_1\\ w_{y2}\\ \varphi_2\end{Bmatrix} \quad (12)$$

in which w_{y1}, φ_1 are the vertical displacement and rotation angle of the left end of girder element, respectively; w_{y2}, φ_2 are the vertical displacement and rotation angle of the right end of element, respectively;

$[M_e]$, $[C_e]$ and $[K_e]$ are the mass matrix, damping matrix and stiffness matrix, respectively;

$$[M_e]=\begin{bmatrix}M_{ww} & M_{wz1} & M_{wz2}\\ 0 & M_{z1z1} & 0\\ 0 & 0 & M_{z2z2}\end{bmatrix}\quad[C_e]=\begin{bmatrix}C_{ww} & 0 & 0\\ 0 & C_{z1z1} & C_{z1z2}\\ C_{z2w} & C_{z2z1} & C_{z2z2}\end{bmatrix}$$
$$[K_e]=\begin{bmatrix}K_{ww} & 0 & 0\\ 0 & K_{z1z1} & K_{z1z2}\\ K_{z2w} & K_{z2z1} & K_{z2z2}\end{bmatrix} \quad (13)$$

$$M_{z1z1}=\begin{bmatrix}m_{11} & & & & \\ & m_{12} & & 0 & \\ & & \cdots & & \\ & & & m_{1i} & \\ & 0 & & \cdots & \\ & & & & m_{1n}\end{bmatrix}_{(n\times n)} \quad (14)$$

$$M_{z2z2}=\begin{bmatrix}m_{21} & & & & \\ & m_{22} & & 0 & \\ & & \cdots & & \\ & & & m_{2i} & \\ & 0 & & \cdots & \\ & & & & m_{2n}\end{bmatrix}_{(n\times n)} \quad (15)$$

$$M_{wz1}=P.M_{z1z1};\ M_{wz2}=P.M_{z2z2} \quad (16)$$

$$P=\begin{bmatrix}P_{11} & P_{12} & \cdots & P_{1i} & \cdots & P_{1n}\\ P_{21} & P_{22} & \cdots & P_{2i} & \cdots & P_{2n}\\ P_{31} & P_{32} & \cdots & P_{3i} & \cdots & P_{3n}\\ P_{41} & P_{42} & \cdots & P_{4i} & \cdots & P_{4n}\end{bmatrix}_{(n\times n)} \quad (17)$$

$$P_i=\begin{Bmatrix}P_{1i}\\ P_{2i}\\ P_{3i}\\ P_{4i}\end{Bmatrix}=\frac{\xi_i(t)}{L^3}\begin{Bmatrix}(L+2x_i).(L-x_i)^2\\ L.x_i.(L-x_i)^2\\ x_i^2.(3L-2x_i)\\ L.x_i^2.(x_i-L)\end{Bmatrix} \quad (18)$$

$$C_{z1z1}=\begin{bmatrix}d_{11} & & & & \\ & d_{12} & & 0 & \\ & & \cdots & & \\ & & & d_{1i} & \\ & 0 & & \cdots & \\ & & & & d_{1n}\end{bmatrix}_{(n\times n)} \quad (19)$$

$$C_{z2}=\begin{bmatrix}d_{21} & & & & \\ & d_{22} & & 0 & \\ & & \cdots & & \\ & & & d_{2i} & \\ & 0 & & \cdots & \\ & & & & d_{2n}\end{bmatrix}_{(n\times n)} \quad (20)$$

$C_{z1z2} = C_{z2z1} = -C_{z1z1}$; $C_{z2z2} = C_{z1z1} + C_{z2}$; $C_{z2w} = (-N_i.C_{z2})^T$ (21)

$$N_i=\begin{bmatrix}N_{11} & N_{12} & \cdots & N_{1i} & \cdots & N_{1n}\\ N_{21} & N_{22} & \cdots & N_{2i} & \cdots & N_{2n}\\ N_{31} & N_{32} & \cdots & N_{3i} & \cdots & N_{3n}\\ N_{41} & N_{42} & \cdots & N_{4i} & \cdots & N_{4n}\end{bmatrix}_{(n\times n)} \quad (22)$$

$$\left.\begin{aligned}N_{1i}&=\frac{1}{L^3}.\left(L^3-3Lx_i^2+2x_i^3\right)\\ N_{2i}&=\frac{1}{L^2}.\left(L^2x_i-2Lx_i^2+x_i^3\right)\\ N_{3i}&=\frac{1}{L^3}.\left(3Lx_i^2-2x_i^3\right)\\ N_{4i}&=\frac{1}{L^2}.\left(x_i^3-Lx_i^2\right)\end{aligned}\right\} \quad (23)$$

International Journal of Engineering Research & Technology (IJERT)
ISSN: 2278-0181
Vol. 6 Issue 06, June - 2017

$[M_{ww}]$, $[C_{ww}]$ and $[K_{ww}]$ are mass, damping and stiffness matrices of the girder elements, respectively. They can be found in Zienkiewicz [14]

$$K_{z1z1} = \begin{bmatrix} k_{11} & & & & \\ & k_{12} & 0 & & \\ & & \cdots & & \\ & & & k_{1i} & \\ & 0 & & \cdots & \\ & & & & k_{1n} \end{bmatrix}_{(n\times n)} \quad (24)$$

$$K_{z2} = \begin{bmatrix} k_{21} & & & & \\ & k_{22} & 0 & & \\ & & \cdots & & \\ & & & k_{2i} & \\ & 0 & & \cdots & \\ & & & & k_{2n} \end{bmatrix}_{(n\times n)} \quad (25)$$

$$K_{z1z2} = K_{z2z1} = -K_{z1z1};\ K_{z2z2} = K_{z1z1} + K_{z2} \quad (26)$$

$$K_{z2w} = -(N_i.K_{z2})^T - (\dot{N}_i.C_{z2})^T \quad (27)$$

$$F_w = \sum_{i=1}^{N}\left[G_i.\sin\psi_i - (m_{1i}+m_{2i})g\right]P_i \quad (28)$$

$$F_{z1} = \begin{Bmatrix} G_1.\sin\Psi_1 - m_{11}.g \\ \vdots \\ G_i.\sin\Psi_i - m_{1i}.g \\ \vdots \\ G_N.\sin\Psi_N - m_{1n}.g \end{Bmatrix}; \quad (29)$$

$$F_{z2} = \begin{Bmatrix} -m_{21}.g + k_{21}.r_1 + d_{21}.\dot{r}_1 \\ -m_{22}.g + k_{22}.r_2 + d_{22}.\dot{r}_2 \\ \ldots \\ -m_{2i}.g + k_{2i}.r_i + d_{2i}.\dot{r}_i \\ -m_{2n}.g + k_{2n}.r_n + d_{2n}.\dot{r}_n \end{Bmatrix}_{n\times 1} \quad (30)$$

Eq.10 can be solved by means of the direct step-by-step integration method based on Runge-Kutta-Mersion method to obtain responses of girder elements.

III. RANDOM ROAD UNEVENNESS

Assume that the PSD (Power spectral density) roughness represented by the angular frequency of a pavement section is known as $S_r(\omega)$. According to Shinozuka [15], Honda [3] and Sun [16] the temporal random excitation formed by a road unevenness can be expressed by means of :

$$r(t) = \sum_{k=1}^{M} A_k \cos(\omega_k t + \Phi_k) \quad (31)$$

where M is a positive integer and Φ_k is an independent random variable with uniform distribution at range $[0,2\pi)$. Also, the discrete frequency ω_k is given by:

$$\omega_k = \omega_1 + \left(k - \frac{1}{2}\right)\Delta\omega \quad (32)$$

in which frequency interval $\Delta\omega=(\omega_m-\omega_l)/M$ and $[\omega_l,\omega_m]$ is the range of frequency where $S_r(\omega)$ has significant values. The amplitude A_k in Eq. (31) is represented by:

$$A_k = \sqrt{2S_r(\omega_k)\Delta\omega} = \sqrt{2S_r(\Omega_k)\Delta\Omega} \quad (33)$$

in which $S_r(\Omega_k)=v.S_r(\omega)$ is the PSD roughness in terms of wave number,Ω, which represents spatial frequency; v is vehicle velocity. From ISO 8608:1995 [1], the PSD roughness in terms of wave number Ω are described by:

$$S_r(\Omega) = S_r(\Omega_0)\left(\frac{\Omega}{\Omega_0}\right)^{-\gamma} \quad (34)$$

where the fix-datum wave number Ω_0 is set as $1/2\pi$ cycle/m. The measurement shows that various values exist for exponential γ and the so-called roughness coefficient $S_r(\Omega_0)$, ranging from 1.5 to 3.0 for γ and from 2×10^{-6} m^3/cycle to 8192×10^{-6} m^3/cycle for $S_r(\Omega_0)$. These different values reflect the components of wavelength in elevation fluctuation and surface condition. Eq. (34) is used as PSD road unevenness later on to generate random road profile. The values of roughness coefficient $S_r(\Omega_0)$ are classified by ISO 8608:1995 in Table 1.

Table 1: Road roughness values classified by ISO 8608:1995

Road class	roughness coefficient $S_r(\Omega_o)$ [10^{-6} m^2/(cycle/m)]		
	lower limit	geometric mean	upper limit
A (very good)	-	16	32
B (good)	32	64	128
C (average)	128	256	512
D (poor)	512	1024	2048
E (very poor)	2048	4096	8192

IV. ANALYSIS RANDOM VIBRATION OF NGUYENTRIPHUONG BRIDGE

A. Properties of structural bridge and vehicle

NguyenTriPhuong bridge located in Danang city, Vietnam. The approach bridge of Nguyen-Tri-Phuong Bridge, which is a two-span slab beam prestressed concrete. The deck of slab beam is connected in the flexible joint between two span, shown in Fig.1. The cross section of the prestressed concrete slab beam and position of vehicle is shown in Fig.3. The three-axle vehicle used in the numerical simulation and the field test is FOTON dumper truck as shown in Fig. 4.

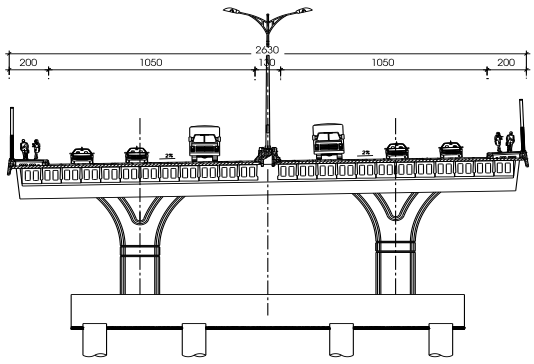

Fig 3. Cross section of slab beam

International Journal of Engineering Research & Technology (IJERT)
ISSN: 2278-0181
Vol. 6 Issue 06, June - 2017

Fig 4. The FOTON dumper truck

The properties of slab beam are collected from design documents of the bridge management unit; the properties of three-axle dumper truck FOTON are given by the manufactory company and checked on site. The parameters of slab beam and dumper truck are listed in Table 2

Table 2. Properties of slab beam and dumper truck FOTON

Item	Notation	Unit	Value
Slab beam concrete			
Lenght	L	m	22.35
Young's modulus	E	Gpa	36
Density	ρ	kg/m^3	2500
Coefficient of internal friction	θ	-	0.027
Coefficient of external friction	β	-	0.01
Cross sectional área	A	m^2	0.723
Second moment of area	I	m^4	0.097
Link slab (deck)			
Height	h	m	0.15
Cross sectional area	A	m^2	0.15
Second moment of area	I	m^4	0.28x10^{-3}
Dumper truck vehicle			
Mass m_{11}	m_{11}	kg	5200
Mass m_{21}	m_{21}	kg	260
Mass m_{12},m_{13}	m_{12},m_{13}	kg	8900
Mass m_{22},m_{23}	m_{22},m_{23}	kg	870
Suspensions spring k_{11};k_{12};k_{13}	k_{1i}	N/m	2.6x10^6
Tires spring k_{21};k_{22};k_{23}	k_{2i}	N/m	3.8x10^6
Suspensions dashpot d_{11};d_{12};d_{13}	d_{1i}	Ns/m	4000
Tires dashpot d_{21};d_{22};d_{23}	d_{2i}	Ns/m	8000

B. *Numerical results*

Base on the survey on site, assume that the road surface condition of Nguyen-Tri-Phuong bridge is Grade C-road (ISO 8608:1995): roughness coefficient Sr(Ω−0)= 256×10−6 m3/cycle; exponential γ=2; M=1000; the range of spatial frequency (wave number) Ωk = [0.011÷2.83] cycle/m. Monte-Carlo simulation method is applied to generate road unevenness profiles. Some of random road unevenness profiles are described as follows:

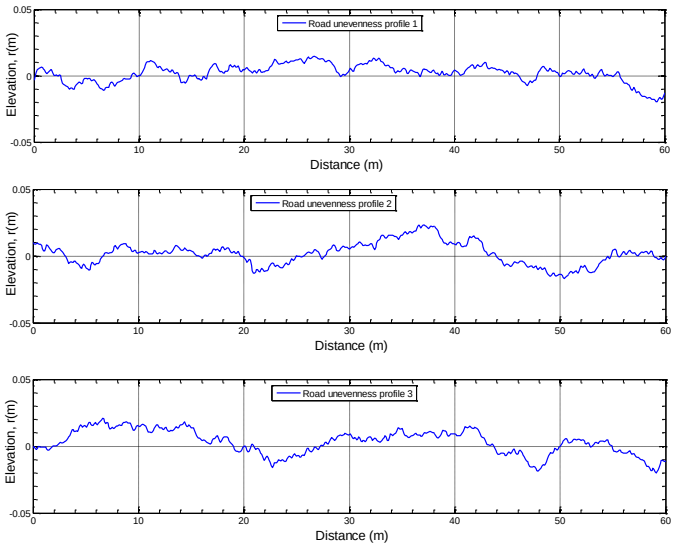

Fig 5. Typical random road unevenness profiles

Using the finite element method, the bridge structure was discrete as Fig.6. The deck of slab beam prestressed concrete are connected in the flexible joint with 1.4m of length. Setting vehicle velocity moving on the bridge is 10 m/s. For each road unevenness input, Eq. 10 is solved by the Runge-Kutta-Mersion method to obtain the static and dynamic displacements of slab beam, shown in Fig.7.

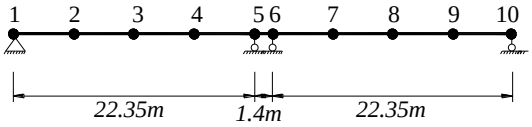

Fig 6. Schematic of discrete bridge structure

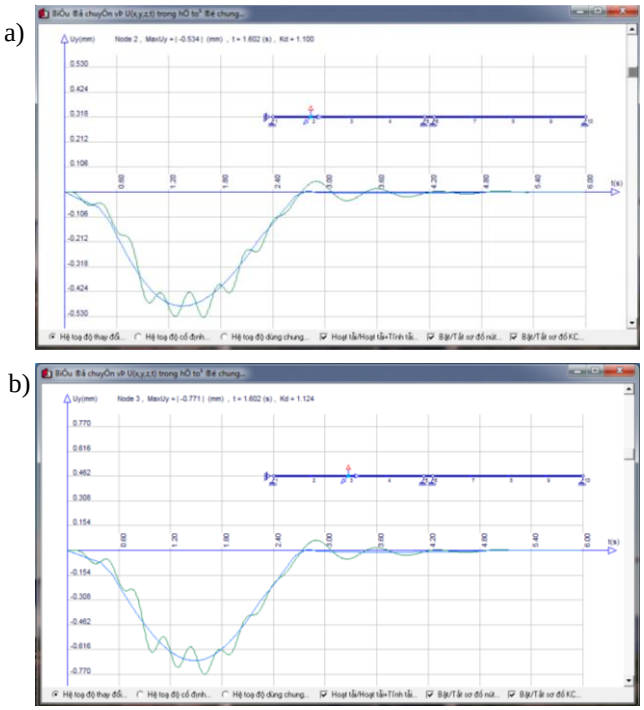

Fig 7. Static and dynamic displacement of 1st span: a) ¼ of 1st span; b) ½ of 1st span

From the time history of 1st span displacements in Fig.7. it can be seen that displacements of 1st span decreased quickly when the dumper truck went over the 1st span. The cause for that

International Journal of Engineering Research & Technology (IJERT)
ISSN: 2278-0181
Vol. 6 Issue 06, June - 2017

issue is that bending stiffness of concrete link slab in the flexible joint is very smaller than bending stiffness of slab beam prestressed concrete.

C. Field measurement results

In order to validate the numerical results, field measurement of dynamic response of slab beam prestressed concrete was conducted at Nguyen-Tri-Phuong bridge in Danang city, Vietnam. This section presents a measurement system and results obtained so far.

Since large vibration of slab beam prestressed concrete had been observed, displacement sensors (LVDT) were placed on ½ of 1st span as Fig.8.

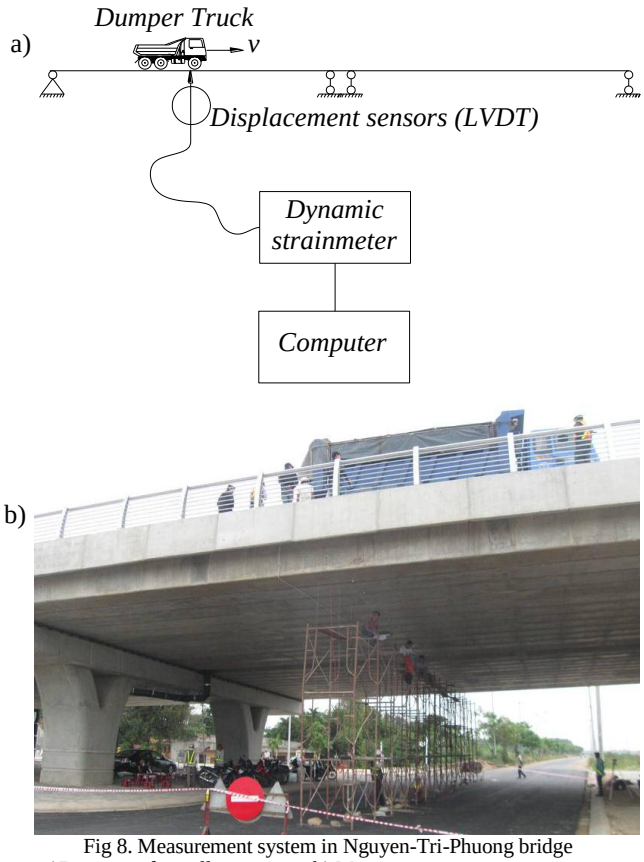

Fig 8. Measurement system in Nguyen-Tri-Phuong bridge
a)Diagram of installing system; b) Measurement system on site

Slab beam vibration was measured after the slab beam was excited by a dumper truck with various velocity. Properties of slab beam prestressed concrete and dumper truck FOTON are listed in Table 2. Since traffic velocity have been limited by the bridge management company, the testing velocity of dumper truck was suggested 10, 20,30 and 40 km/h. For each velocity level of testing vehicle, dynamic displacement of slab beam prestressed concrete was recorded and compared with the numerical results, shown in Fig.9

From the time history of 1st midspan displacement in Fig.9, it can be seen that the numerical results (FEM results) show quite good agreement with the experiment results at the field. The difference of maximum dynamic displacement between them are 3.83%; 4.77%, 5.24% and 6.12%, respectively with the moving vehicle velocity 10, 20, 30 and 40 km/h. Therefore, the algorithm and numerical model mentioned above are quite reliable. This numerical model are used continuously to investigate the influence of the road surface condition on dynamic impact factor of slab beam prestressed concrete in the next section.

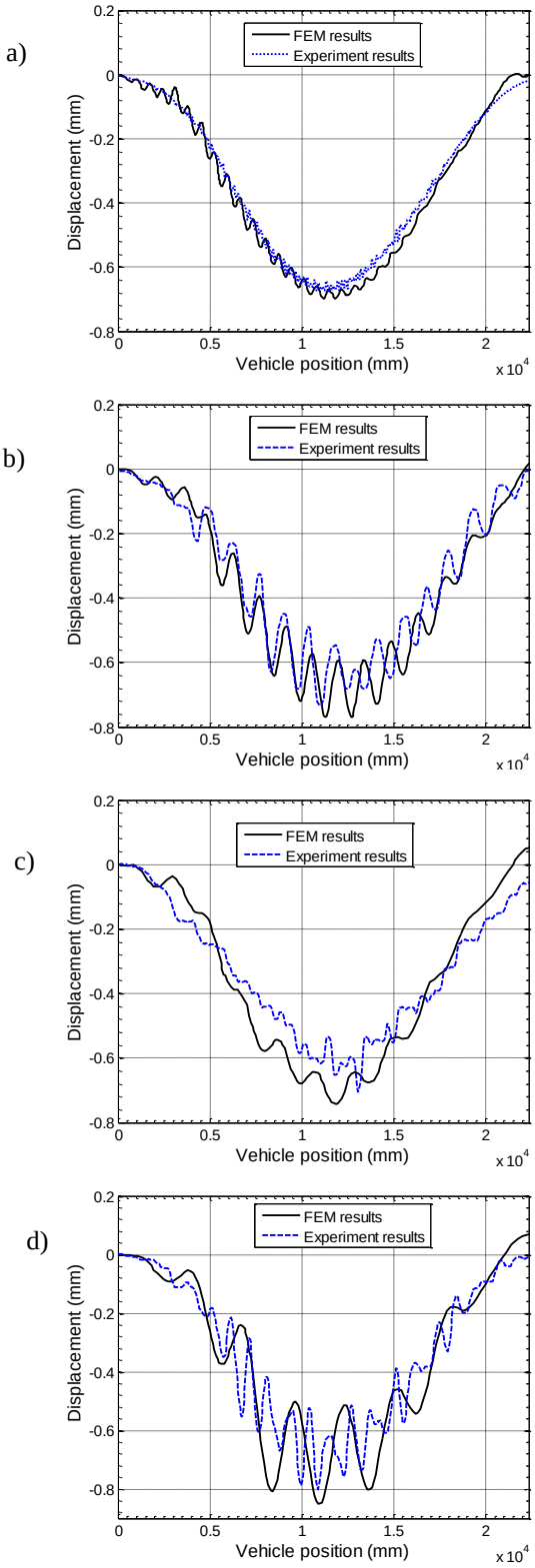

Fig 9. Time history of displacement at 1st midspan: a) v=10 km/h; b) v=20 km/h; c) v=30 km/h; d) v=40 km/h

International Journal of Engineering Research & Technology (IJERT)
ISSN: 2278-0181
Vol. 6 Issue 06, June - 2017

D. Numerical investigation

Base on the validated numerical model with experiment results above, it carried out to investigate dynamic vehicle-bridge interaction for this numerical model with various road surface condition. Assume that the roughness coefficient changed in the range, $S_r(\Omega_0)$ = [0, 32, 128, 512, 2048, 8192]×10^{-6} m^3/cycle, corresponding to the road surface condition: ideal smooth, Grade A, B, C, D and E (ISO 8608:1995). The velocity of dumper truck was 10 m/s. The other parameters of structural bridge and dumper truck vehicle was given as Table.2. For each the road surface condition, Monte-Carlo simulation method is applied to generate 100 road unevenness profiles. With each road profile input, the governing equation of vehicle-bridge interaction is solved to obtain static and dynamic displacements output of slab beam concrete. From static and dynamic displacement, it can determine dynamic impact factor of slab beam prestressed concrete as shown in Eq.35:

$$(1+IM)_x^j = \frac{R_D^j(x)}{R_s^j(x)} \qquad (35)$$

where $R^j_D(x)$ is the dynamic displacement of slab beam prestressed concrete at position x due to dumper truck moving on j^{th} road unevenness profile; $R^j_s(x)$ is the static displacement of slab beam prestressed concrete at position x due to dumper truck moving on j^{th} road unevenness profile.

After analyzing with a series of road profiles input, it can obtain a series of dynamic impact factor output which are also random process as shown in Fig.10. The statistical characteristics of the dynamic impact factor (IM) at 1st midspan are described in Table 3.

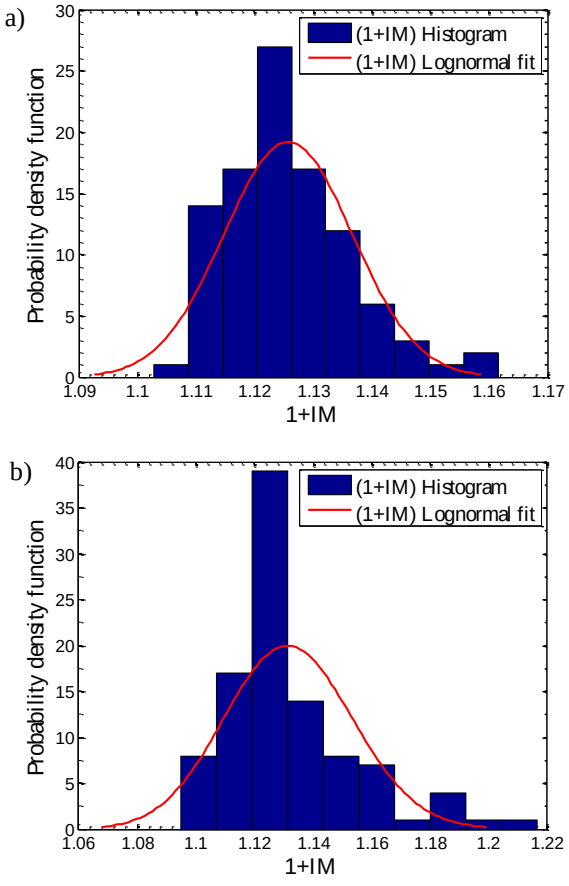

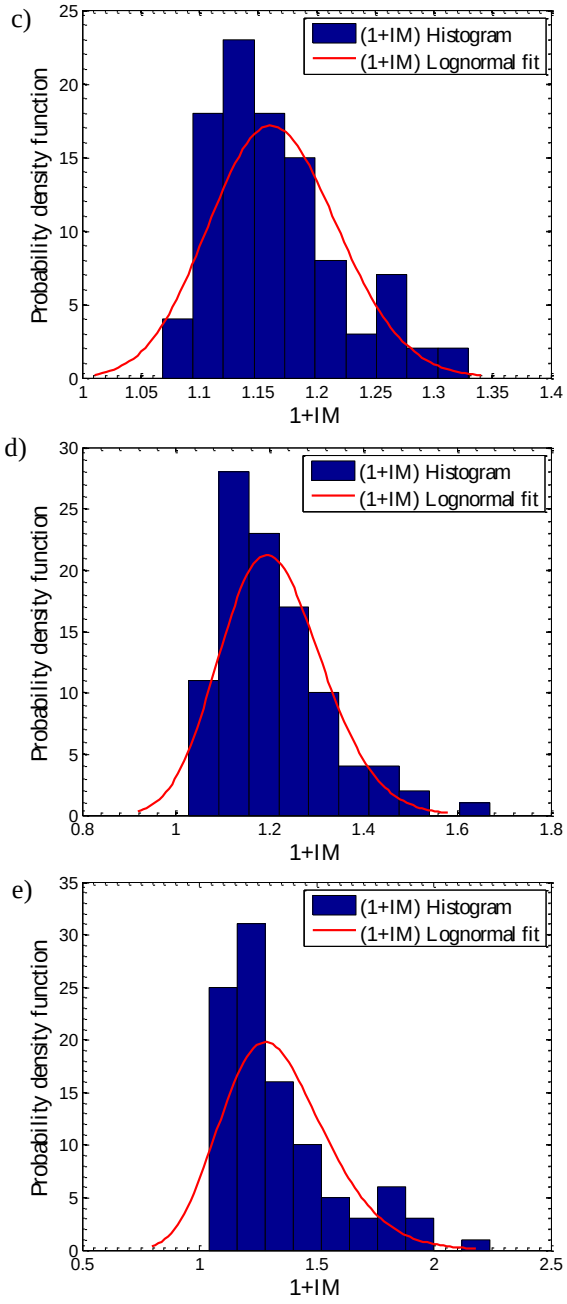

Fig 10. Dynamic impact factor at 1st midspan due to dumper truck: a) grade A-road; b) grade B-road; c) grade C-road; d) grade D-road; e) grade E-road

Table 3. Statistical characteristics of dynamic impact factor at 1st midspan

$S_r(\Omega_0)$ x10^{-6} m^3/cycle	Dynamic Impact Factor (1+IM)			
	Mean	Max	Min	Standard deviation
0	1.12	-	-	-
32	1.126	1.159	1.093	0.019
128	1.134	1.199	1.068	0.038
512	1.175	1.34	1.011	0.096
2048	1.249	1.579	0.918	0.194
8192	1.488	2.18	0.796	0.405

International Journal of Engineering Research & Technology (IJERT)
ISSN: 2278-0181
Vol. 6 Issue 06, June - 2017

Base on statistical characteristics of IM in Table.3, the relationship between the mean value of IM and the road unevenness condition can be established in Fig 11. In the Fig.11, the correlation equation between the mean value of IM and road surface condition are also found out, in which x is the roughness coefficient.

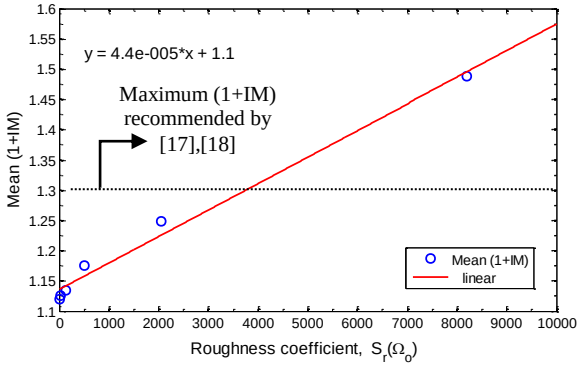

Fig 11. Mean value of IM versus the roughness coefficient

From the investigation results in Fig.11, it can be seen that when the road surface condition changes to be grade A-road, grade B-road, grade C-road the mean value of IM increases 0.54%, 1.25% and 4.91%, respectively. Specially, the mean value of IM reaches 11.52% and 32.85%, respectively, while the road surface condition changes to be grade D-road and grade E-road. This increase in dynamic impact factors are quite large and exceed those recommended by current bridge design codes as AASHTO [17] and Vietnamese Specification for Bridge Design [18]. Therefore, it is necessary to consider the influence of road surface condition on analyzing dynamic response of structural bridge, especially bridges have passed long time in operation and the pavement have been damaged as well as seriously downgraded.

V. CONCLUSIONS

In this paper, the analysis of random dynamic interaction between three-axle dumper truck vehicle and two-span slab beam prestressed concrete with link slab due to road unevenness is investigated by means of finite element method and Monte-Carlo simulation method. The road unevenness are described by a zero-mean stationary Gaussian random process. The bridge is modeled by finite element method. The dumper-truck has three axles. Each axle is idealised by two mass, in which a mass is supported by a spring and dashpot. The governing equation of random dynamic vehicle-bridge interaction is derived by means of dynamic balance principle. Galerkin method and Green theory are employed to discrete the governing equation in space domain. The solutions of governing equation are solved by Runge-Kutta-Mersion method in time domain. Monte-Carlo simulation is applied to generate the random road unevenness input. The numerical results are in good agreement with full-scale testing results at Nguyen-Tri-Phuong bridge in Danang city, Vietnam. In addition, this research evaluates the effects of the road surface condition on dynamic impact factor of slab beam prestressed concrete. The numerical results showed that the road surface condition has significantly effects on dynamic impact factor of slab beam prestressed concrete. Specially, the mean value of IM reaches 32.85%, respectively, while the road surface condition changes to be grade E-road. This value of dynamic impact factors are quite large and exceed those recommended by current bridge design codes. Therefore, it is necessary to consider the influence of road surface condition on analyzing dynamic response of structural bridge subjected to moving vehicles, especially bridges have passed long time in operation and the pavement have been damaged as well as seriously downgraded.

REFERENCES

[1] ISO 8608:1995 ‘‘Mechanical vibration – Road surface profiles – Reporting of measured data’’ issued by the *International Organization for Standardiazation* (ISO).
[2] Frýba, L. (1996).*Dynamics of railway bridges*, Thomas Telford, London.
[3] Honda, H.,Kajikawa, Y., and Kobori, T. (1982). “Spectral of road surface roughness on Bridges”. *ASCE of Structural of the Division*, 108(9): 1956-1966.
[4] Palamas, J., Coussy, O., and Bamberger, Y. (1985). “Effects of surface irregularities upon the dynamic response of bridges under suspended moving loads”. *Journal of Sound and Vibration*, 99(2): 235-245.
[5] Coussy, O., Said, M., and Van Hoore, J.P. (1989). “The influence of random surface irregularities on the dynamic response of bridges under suspended moving loads”. *Journal of Sound and Vibration*, 130(2): 3 13-320.
[6] Inbanathan, M.J., and Wieland, M. (1987). “Bridge vibrations due to vehicle moving over rough surface”. *ASCE Journal of Structural Engineering*, 113(9): 1994-2008.
[7] Hwang, E.S., Nowak, A.S. (1991). “Simulation of dynamic load for bridges”. *ASCE Journal of Structural Engineering*, 117(5): 1413-1434.
[8] F.T.K Au, Y.S. Cheng, Y.K. Cheung. (2001). “Effects of random road surface roughness and long-term deflection of prestressed concrete girder and cable-stayed bridges on impact due to moving vehicles”, *Computer and structures* 79 (2001) 853-872.
[9] Geert Lombaert and Joel P. Conte. (2012). “Random vibration analysis of Dynamic Vehicle-Bridge interaction due to Road Unevenness”. *Journal of Engineering Mechanics*.2012. 138:816-825.
[10] Toan X.N, Duc V.T (2014). “A finite element model of vehicle - cable stayed bridge interaction considering braking and acceleration”. The 2014 World Congress on Advances in Civil, Environmental, and Materials Research. Busan, Korea. P.109(20p.)
[11] Toan, X.N. (2014), “Dynamic interaction between the two axle vehicle and continuous girder bridge with considering vehicle braking forces”, Vietnam Journal of Mechanics, vol 36, p49-60.
[12] Xuan-Toan Nguyen, Van-Duc Tran, Nhat-Duc Hoang. (2017) “A Study on the Dynamic Interaction between Three-Axle Vehicle and Continuous Girder Bridge with Consideration of Braking Effects”. *Journal of Construction Engineering*, Volume 2017 (2017), Article ID 9293239, 12 pages.
[13] Ray, W. C., and Joseph, P. (1995). *Dynamics of structures*. 3rd Ed. Computers & Structures, Berkeley, California .
[14] O.C. Zienkiewicz, R.L. Taylor, J.Z. Zhu. *The Finite Element Method: Its Basis and Fundamentals*, Seventh Edition. Butterworth-Heinemann, 2013.
[15] M. Shinozuka, Digital simulation of random processes and its applications, *J. Sound Vib*. 25 (1972) 111–128.
[16] L. Sun, “Simulation of pavement roughness and IRI based on power spectral density”, *Mathematics and Computers in Simulation* 61(2003) 77–88.
[17] AASHTO, *LRFD Bridge Design Specifications*, AASHTO, Washington, DC, USA, 2012.
[18] Vietnammese Specification for Bridge Design, 2005. 22TCN 272-05.